Wing Sweeping Mechanism for Active Control and Stabilisation of a Flapping Wing MAV

Olejnik, Diana; Sujit, Aadithya; Karasek, Matej; Remes, Bart; de Croon, Guido

Publication date
2018

Document Version
Final published version

Published in
10th International Micro-Air Vehicles Conference

Citation (APA)
Olejnik, D., Sujit, A., Karasek, M., Remes, B., & de Croon, G. (2018). Wing Sweeping Mechanism for Active Control and Stabilisation of a Flapping Wing MAV. In S. Watkins, & A. Mohamed (Eds.), *10th International Micro-Air Vehicles Conference: 22nd-23rd November 2018. Melbourne, Australia* (pp. 120-126)

Important note
To cite this publication, please use the final published version (if applicable).
Please check the document version above.

Wing Sweeping Mechanism for Active Control and Stabilisation of a Flapping Wing MAV

Diana Olejnik *, Aadithya Sujit †, Matej Karasek, Bart Remes, Guido de Croon
MAVlab, Control and Operations, Faculty of Aerospace Engineering, TU Delft

ABSTRACT

During flight, natural fliers flap, twist and bend their wings to enhance flight performance. Lift and thrust benefit from flexibility as well as from both passive and active wing deformation. At the same time, the active deformations are used for flight control. In this study, we investigate strategies of control moments generation in a bio-inspired flapping-wing micro air vehicle (FWMAV). In particular, we propose a method for active control and attitude stabilization by introducing a wing deformation through adjustable wing sweep. The control method is demonstrated on a tailless FWMAV with independent wing sweep modulation on each of its four wings. The actuation mechanism consists of an arm joint at the leading edge, about which the wings are swept. Forces from the servo actuation are transferred to the leading edge of the robot through strings. The actuated strings alter the wing sweep, which affects the roll and pitch movement via different combinations of string pulls. The effectiveness of the designed mechanism is being evaluated on the basis of tethered force balance tests and free flight tests. An advantage of the proposed mechanism is its lightweight design, which is crucial for small FWMAVs with stringent weight restrictions.

1 INTRODUCTION

Diversity in environmental conditions have forced airborne animals to perfect their flight manoeuvres. Many natural flyers rely on wing morphing to achieve various flight maneuvers such as making swift turns or dodging an obstacle. During flapping, birds tend to fold their wings at the beginning of upstroke to reduce the counter productive forces by not only decreasing their wing area [1], but also reducing the inertial forces [2]. Furthermore, a re-configurable wing geometry allows changing the lift and drag coefficients. Gliding birds in particular take advantage of their swept wings at high gliding speeds to minimize drag [3], but during take-off and landing, their extended wings maximize drag and lift accordingly [4]. Morphed wings can also produce lower aerodynamic load, decreasing the risk of flow separation [5, 6].

The idea of wing morphing has encouraged many UAV (Unmanned Aerial Vehicle) researchers to design aircraft and bio-inspired prototypes of aerial robots that enable wing morphing by either altering the profile or planform of the wing [7, 8, 9]. Inspired by bats and birds, Stowers [10] has adapted passive wing morphing by introducing a mechanism with wrist joints to fold and unfold the wing. This research has also led to a great contribution to the understanding of the physics of wing morphing. RoboSwift, a MAV that mimicks the agile swift bird, uses active wing sweep to ensure highly efficient gliding flight at various flight speeds [11]. The prototype can quickly change its wing area, sweep, slenderness and camber by folding its "feathers" backward while its flight control and stability is maintained with use of a tail.

The development of tail-less flapping wing MAVs that use morphed wings for control is even more challenging. For instance, BatBot is equipped with the multiple-degree-of-freedom wings which are covered using a flexible membrane [12] in order to enhance the number of possible maneuvers. However, the complex actuation mechanism represents a significant weight penalty. Due to limited lift production, the vehicle's flight maneuvering capabilities could only be demonstrated in fast forward, descending flight. The Nano Hummingbird by Keennon [13] uses the concept of wing twist modulation and rotation to achieve control and stability of the robot. The prototype also demonstrates an outstanding flight performance and maneuverability, allowing hovering as well as fast forward flight. However, the mechanism used to control the Hummingbird is highly complex. Several more recent designs lead to successful flight, but with less complex mechanisms [14, 15]. In terms of complexity, arguably the simplest design, dubbed "quad-thopter", was introduced in [16]. The quad-thopter is named after the quadrotor, where the rotors are replaced by (in this case double) wings. The design and control of this vehicle is rather straightforward. However, there is a weight and miniaturization penalty involved in having 4 gearboxes, motors, etc. Despite the successes in the literature, the search for straightforward, lightweight and high-performance control designs continues, also with further miniaturization in mind.

Regardless of the different designs, as of yet, there is no existing flapping wing MAV that utilizes swept wing technique to achieve autonomous flight. In this article, we present a tailless FWMAV that uses a novel method to attain flight

*D.A.Olejnik@tudelft.nl
†aadithyasujit@gmail.com

control by means of a wing sweep deformation technique. The system benefits from simplicity arguably, the motor just provides propulsion, and a servo the attitude control.The prototype is equipped with an autopilot for active stabilization and an autonomous flight. The FWMAV design is based on the Delfly flapping-wing vehicle developed at TU Delft [17]. We have kept its reliable flapping mechanism, but adjusted the leading edge design such that they can be bent by servo-actuated strings. The employed solution eliminates the need for a tail or any other additional control surfaces such as an elevator or rudder, thereby ensuring a lightweight design and reduction in the size of the FWMAV. By means of wing deformation, control moments can be actively generated and the developed MAV can exhibit close to hover flight. Preliminary tests show the capability of stable flight for 12 seconds.

2 Design and Materials

The starting point of this research is the Delfly bio-inspired MAV that can fly forward, backward for a short duration and even hover. Two actuated control surfaces on the conventional tail, the elevator and rudder generate the pitching and a combined yawing and rolling moments respectively. Due to the tailed design, this platform benefits from passive stability. A characteristic feature of the vehicle is the clap-and-peel mechanism of wings which induces additional thrust. For a more detailed information of the Delfly Project, the reader is referred to de Croon et al. (2016) [18].

Since the Delfly has proven to be a reliable platform allowing repeatable experiments, further development of the platform is mainly focused on the improvements that can be easily integrated with the existing MAV and allow to improve its controllability or limit power requirements. Here we present a tailless FWMAV (Figure 1) with bio-inspired wing sweep actuation mechanism.

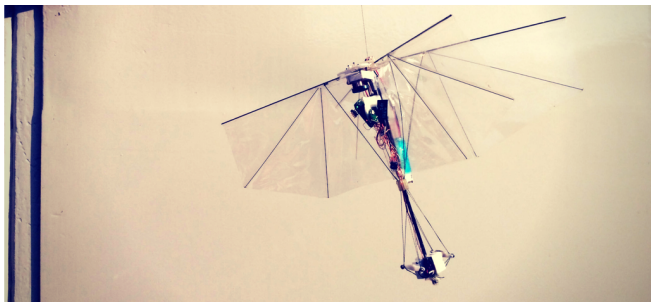

Figure 1: The proposed tailless flapping wing MAV with bio-inspired wing sweep actuation mechanism.

The prototype is equipped with a Lisa MXS autopilot [1], which consist of a 168 MHz STM32F4 microprocessor with 1 MB of flash memory. The board provides features such as a pressure sensor and three-axis gyros, accelerometers and magnetometers. To restrict the influence of the high frequency vibration and noise, polyurethane foam and depron were placed between the autopilot and the fuselage. The active stabilization and control are handled through the open-source autopilot software, Paparazzi UAV [2]. The pilot's commands are collected via radio link by DelTang Rx31 micro receiver. The Mi-3A brushless electronic speed controller (ESC), flashed with BLHeli firmware, is used to drive the BLDC motor. A pair of rotational servos (HobbyKing HK-5330 Ultra-Micro Digital Servo) capable of producing a torque up to 0.17kg is used as actuators, these actuators are coupled to their respective wing/wing pairs by means of low stretch string. This string has a line thickness of 0.12 mm and is made from Dyneema fibres making it ideal for high power pulling application without stretching. A high density-low weight Turnigy nano-tech LiPo battery with a 160 mAh capacity is used as the energy source for the system of electronics.

2.1 Design Concepts

In order to achieve greater agility of the prototype, we have come up with two viable solutions that utilize the wing sweeping technique to control the attitude of the MAV. In the first solution, by taking inspiration from nature, we introduce a wrist joint as a part of the leading edge of the wing which mimics a bat wing morphology (Figure 2). The hinge part was printed using a Multi-Jet Modeling process from a UV-cured acrylic polymer.

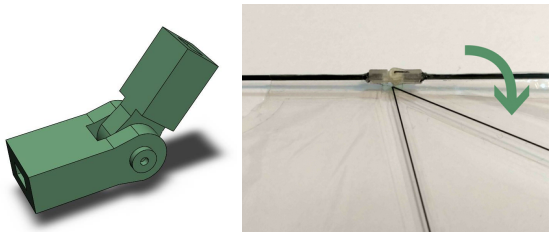

Figure 2: CAD model of the hinge (left), the hinge placed on the leading edge of the wing (right).

The hinge is positioned near the crossing of wing stiffeners at the leading edge. The leading edge carbon rods bend such as to increase wing sweep. In its second version, changes have been made to the structure to enhance the elasticity close to the hinge by adding thin steel rods. This slightly increased the capability of the wings. Downside of the solution is the fragility of resin based materials, which in free flight would be a risk. Due to these problems, decision was made to test another prototype.

An alternate solution to increase the magnitude of deviation along the wing is to vary the stiffness of the leading edge by either changing the cross sectional profile or thickness at a specific location. This section is characterized by decreased stiffness about which the leading edge bends. To achieve this,

[1] https://wiki.paparazziuav.org/wiki/Lisa/MXS_v1.0

[2] http://wiki.paparazziuav.org/

a small slit is milled on the leading edge rod using a CNC machine. The rod is then manually delaminated near the slit and the extent of delamination is restricted using shrink tubes (Figure 3). On testing different lengths of introduced gap, it was found that with increase in length, the required force to actuate the wing is minimized. The downside of an increased length is a faster deterioration of the material. The location of the delaminated section along the leading edge is chosen to be as close as possible to the swing arm (5 mm form the root) so that almost the entire wing can be bent. To externally actuate the wing bending, an actuation system inspired by our previous work on wing tension modulation [19] is used. As shown in figure 4, the system consists of rotational servos and strings that are attached to the leading edges. When the servo arm is actuated, it tensions the string which in turn forces the wing to bend in the desired direction. The advantage of this system being that the servo only needs to pull in one direction. When the servo arm is released, the leading edge naturally unbends itself.

Figure 3: Process of delamination of the carbon fiber rods.

The idea behind the mechanism is that whenever a wing is bent by pulling the strings, that particular wing alters its profile due to slackening. This effect causes the wing to produce less thrust relative to the other wings causing an imbalanced force production thus resulting in a control moment. By means of this mechanism, differential control can be performed by bending the leading edges of the wings for creating moments to control and navigate Delfly. Another effect is that, while bending a wing about its fuselage, the thrust vector is tilted such that it remains perpendicular to the leading edge. This vectoring of thrust on the bent wing can alter the moments generated and direction of the net thrust produced.

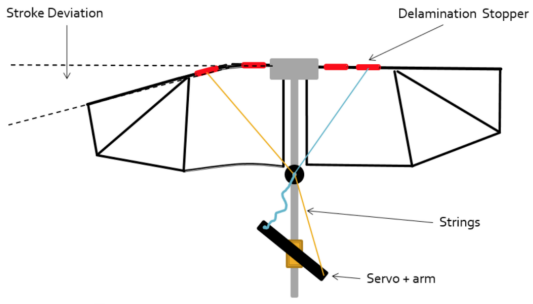

Figure 4: Bending of the leading edge using servo and string based actuation mechanism from the front view.

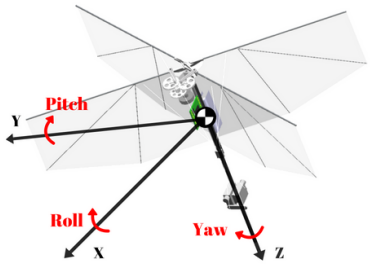

Figure 5: The axis convention used to describe the robot rotations.

To describe the body rotations, we adopt an aerospace coordinate system according to Figure 5. The proposed actuation scheme with differential control of wing bending is shown in Table 1. For instance, when both wings on the left side are actuated, the thrust produced by the actuated pair is significantly lower relative to that of the right side. This difference in thrust produced between the two sides generates a moment about the center of gravity (cg) which steers the flapper to the left side resulting in a left roll. Likewise, pulling the right wing pair will result in a right roll. Similarly, when the bottom wings of either side of the flapper are actuated, the corresponding wing pair loses thrust relative to the top pair, resulting in a moment that pitches the flapper downwards. Likewise, pitching up moment will be generated when the top pair of the wings are actuated. Although our hypothesis does not hold strong for the yaw command, the flapper is expected to generate yaw when the adjacent pair of wing are actuated. The possible reason for this could be that when the wings are actuated, the slackness of the wing causes the foil of the wing to freely flex during one stroke while in the return stroke, the foils deformation is restricted by the string. This alternately occurring phenomena is expected to result in a yaw moment. The clap-and-peel mechanism of wings is less effective for the considered maneuver. The proposed arguments have been proved in by the experimental study shown in Chapter 4.

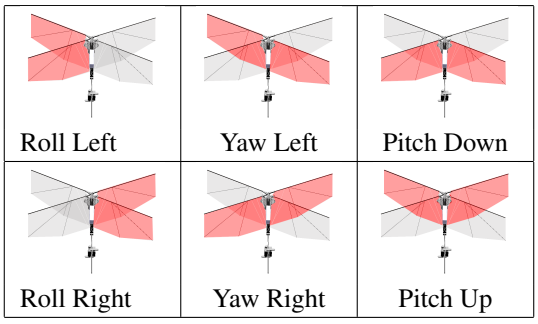

Table 1: Control moments generation scheme with respect to the used combinations of a wing pulling. The flapper is shown from rear view and actuated wings are colored in red.

3 Experimental Setup

To determine and validate the capabilities of the prototype, we performed two tests: tethered and free flight. Further explanation of the experimental setup is presented in the following chapter with main focus on force balance tests.

3.1 Tethered force balance tests

In order to validate the generated moments, the prototype was mounted onto a 6 axis force transducer - ATI Nano-17 Titanium. The measurement setup logs the forces and moments along the 3 axis. Additionally, flapping frequency and power consumption is recorded via measurements of current, voltage, and counting of the brushless motor polarity changes. The flapper was clamped on the force sensor close to the cg in a yz plane.

A servo tester connected to the ESC was used to adjust the flapping frequency. All the experiments were conducted for a range of frequencies varying from 6 z to 20 Hz; the vehicle hovers at about 15 Hz. This assumption is made based on the data of a similar sized MAV used in the past [18]. The data acquisition was handled by the NI cRIO-9024 controller with a FPGA.

Data processing was performed using MATLAB R2017b software. The obtained raw data of forces and moments was filtered using Chebyshev Type II low-pass filter with -80dB attenuation of the stopband. To prevent time shift of data, the forward-backward filtering technique was used via filtfilt function of MATLAB [14]. The 50 Hz cut-off frequency was selected based on assumption that we should keep at least first two harmonics of Z-force power spectral density (Figure 6) due to the suggestion that the two first peaks are related to the aerodynamic forces production [20].

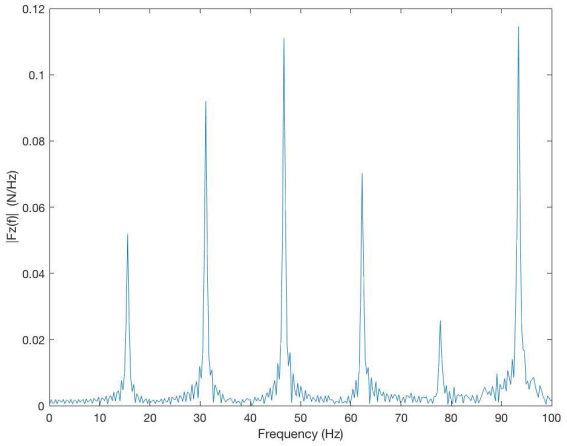

Figure 6: Single-Sided Amplitude Spectrum.

3.2 Free flight test

To achieve stable flight, the attitude of the 19.76-gram prototype was autonomously controlled using a PD controller with attitude feedback from the on-board IMU of the Lisa MXS autopilot. The P and D gains were hand-tuned using a trial and error method, until acceptable performance was achieved. As a starting step, the gains were initialized to the values of similarly sized vehicles and tuned until a stable flight is achieved.

For the power source, a single cell (1S) high density and low weight LiPo battery is used. Two batteries with similar specifications but with varying discharge rates were used for the Delfly in free flight. The position of the battery (being the most significant weight on the prototype) is also very crucial for determining the cg location of the Delfly, which in turn determines the static and dynamic stability [21].

The total moment generated by the flapper depends on the relative distance of the cg and the application point of the acting forces. When the battery was placed at the bottom of the fuselage, the dynamic stability of the flapper improved but the control effectiveness decreased. When a roll or pitch command is given, the normal or side drag force opposing the body motion acts on a large moment arm and results in a significant opposite (counter) moment to that of the desired control moment [22], which decreases the overall effectiveness of the control.

When the battery was placed at the top of the flapper, high control effectiveness was achieved but leaving the system dynamically unstable. Because the moment arm of the body-motion induced drag forces is now in the opposite direction, this drag-based moment is in the same direction as the desired control moment, virtually increasing the control effectiveness, but (statically) destabilizing the system.

In the first flight trials, the vertical location of the battery was being adjusted to find a suitable vertical cg location. We ended up with a battery placed roughly near the quarter chord point, which was a good compromise between effective control and stability, and is in agreement with recommendations based on theoretical models given in [21].

4 Results & Discussion

4.1 Clamped force data

First, the tethered force balance tests have been conducted. The moments, recorded in the force balance reference frame, was transformed to the vehicle cg.

As shown in Figure 7, the flapper produces a mean force Fz of -0.29 N when no actuation of the wing sweeping mechanism is applied. The generated force is sufficient enough to support the flight of the 19.76 gram FWMAV. It can be observed that the mean force Fx is very close to 0 N. This is due to the symmetric flapping motion of the front and rear wings that flap in counter sense, resulting in a cancellation of the Fx force produced by each individual wing. In the hover case (zero free stream), the flapper purely relies on the Fz force to stay in air.

Although we thought that a yaw moment could be generated, the experiment showed no significant yaw moment

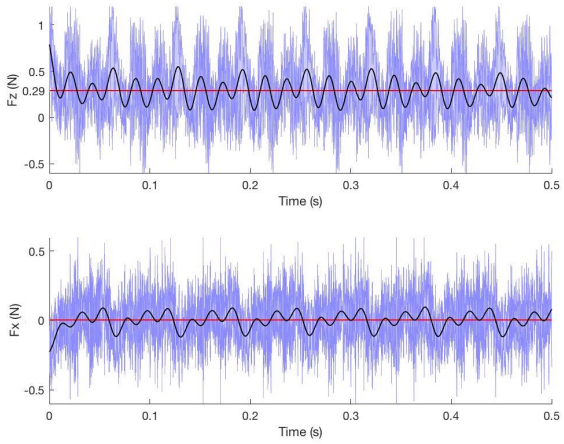

Figure 7: The tethered force balance measurements of Fz and Fx forces. The blue and black lines represents raw and filtered data respectively, while the red line indicates the mean value of the filtered data.

production. When wings were actuated (see Table 1 - yaw maneuver) the flapping frequency of DelFly dropped significantly, losing thrust below the equivalent weight of the DelFly. This was due to increased friction at the cross over region of the swing arms that led to loss of flapping frequency and thrust.

However, the roll (Mx) and pitch (My) moments measurements are generally in good agreement with the assumed scheme of control moments generation. Comparison of rolling and pitching moments characteristics during the flapping motion for different actuations (Table 1 of the swept wings can be seen in Figure 8). For the sake of clear comparison no actuation mode is also displayed.

When the shape of the Fx curve in Figure 7 is closely observed, it can be seen that each flapping cycle consist of two minor peaks and one major peak. When the position of the leading edge was studied using a hall sensor with comparison to the respective forces and moments, it was found that the major peak occurs during the peel action or the outward stroke and the following minor peaks occurs during the the clapping action and possibly at the stroke reversal when the wing flexes pushing more air. For more details, the reader is referred to [14].

This trend is very similar in the Mx moment plot showed in Figure 8, the plot clearly depicts these peaks for no actuation and left actuation and to some extent in the right actuation curve. The possible reason for the absence of third minor peak in the right actuation curve could be due to the interaction of wing and string when actuated does restricts the natural flexing of wing at stroke reversal.

It can be noticed, that the average effective moment generated about the roll axis is higher than pitch axis. Although

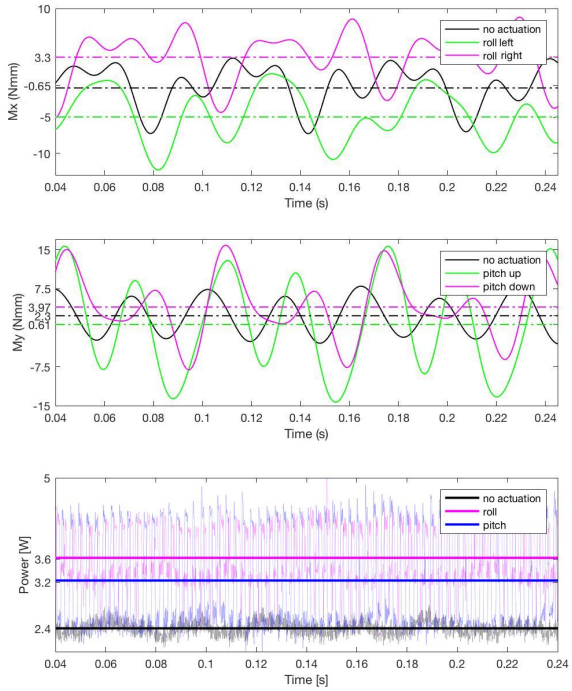

Figure 8: Comparison of rolling and pitching moments characteristics (top and center) and mean average power (bottom) during the flapping motion for different actuation scheme.

the displacements due to actuation for all the 4 independent wings were calibrated to be of same magnitude, and thus have a similar effect on the modulation of each wing's thrust force, the moment arm of the thrust force is larger in the roll case ($L/2cos(\phi/2)$) than in the pitch case ($L/2sin(\phi/2)$), which explains the higher roll moments. Here we assumed that the wing thrust force lies near the mid-span of the wing with a length L, ϕ is the flapping angle measured with respect to the y axis.

4.2 Power Requirements

On testing the power requirements for an actuated and non-actuated system, it was observed that the flapper uses a lot more power when actuated. Although the servo limits were set as to not cause any saturation, the system draws additional current to bend the wing and hold them in the desired position. Additionally, bending of the wing increases the friction between the hinges resulting in increased motor load. This decreases the flapping frequency. In Figure 8, it can be observed that for a given time of 0.25 secs, the actuated plot comprises of three flapping cycles while the non-actuated plot comprises of four flapping cycles. This implies that the actuated wing flaps at 12-13 Hz while a non-actuated wing flaps around 15 Hz. From Figure 8, actuation of flapper increases the power requirement from 2.4 W to 3.6 W. It can also be observed that the roll actuators draw more power

than the pitch due to the design of the swing arm and fuselage interface.

4.3 Flight Testing

For a further confirmation of our findings, we have also performed free flight experiments. During the first test, with a slightly used Hyperion battery (180 mAh) as a power source, for a given input throttle command, the altitude of the Delfly was slowly decreasing with auto stabilization. However without auto stabilization, the Delfly seemed to climb for the same throttle command. This indicates that with the auto stabilization, the system draws more current than the power source can provide. After replacing the power source with the a brand new and 1 gram lighter battery (Turnigy- 160 mAh), the problem of decreasing thrust was addressed. Due to lower mass the current draw has decreased. However, this would reduce the overall flight time due to the lower capacity of the chosen battery. It was also observed that the structural support for the autopilot played a crucial role in achieving a hovering free flight without saturating the on board sensors of the autopilot. Adding a depron and PU foam between the fuselage and the autopilot absorbed most of the noise caused by the vibration of flapper. A standard state estimation and loop within the paparazzi software was used and parameters related to roll and pitch were adjusted. The gains of the controller were tuned to stabilize the attitude of the flapper.

With sufficient current available and a tuned controller, the prototype could self stabilize in hover condition for 12 seconds (the three first frames on Figure 9) while gradually building oscillations and decreasing its altitude indicating loss of thrust (the fourth and fifth frames on Figure 9) due to low battery level. These oscillations of the flapper along the pitch axis indicates insufficient power to the servo actuators. The actuators draw more current either while trying to hold an actuated position or at the extreme actuated position. This results in shortage of power to the motor which eventually decreases the flapping frequency, and results in a loss of thrust (the sixth frame on Figure 9). (The supplementary video is available online at `https://www.youtube.com/playlist?list=PLwJoNhf07bFJefdur7OhHrAzIU3hCMZOq`)

5 Conclusion

Inspired by birds and bat flight we developed a flapping wing MAV that uses wing sweep modulation for active control and stabilization. We carried out the tethered force balance tests and free flight experiments to validate the platform performance as well as to confirm the assumed scheme of control moments generation resulting from actuation of various wing combinations. An advantage of the proposed mechanism is its lightweight design and simplicity.

The objective of future work is to extend this analysis of alternative bending points and possibly design new actuation mechanism that will also allow to generate a yaw moment. The design of the hinge and the sandwiched swing arm configuration can be improved to not only handle larger magnitudes of actuation but also to reduce the frictional loss. Thereby, minimizing the power needed during actuation. In addition, the duration of the final flight time can be increased by looking more into the power management of the system. A possible solution could be to use an independent power source for the actuators to ensure that thrust production is unaffected during extreme actuation.

Figure 9: Time frames of a free flight test.

Acknowledgements

This work is part of the Open Technology Programme with project number 15039, which is financed by the Netherlands Organisation for Scientific Research (NWO).

NWO Netherlands Organisation for Scientific Research

References

[1] Florian T Muijres, Melissa S Bowlin, L Christoffer Johansson, and Anders Hedenström. Vortex wake, downwash distribution, aerodynamic performance and wingbeat kinematics in slow-flying pied flycatchers. *Journal of The Royal Society Interface*, 9(67):292–303, 2012.

[2] Daniel K Riskin, Attila Bergou, Kenneth S Breuer, and Sharon M Swartz. Upstroke wing flexion and the inertial cost of bat flight. *Proceedings of the Royal Society of London B: Biological Sciences*, 279(1740):2945–2950, 2012.

[3] D Lentink, UK Müller, EJ Stamhuis, R De Kat, W Van Gestel, LLM Veldhuis, Per Henningsson, Anders Hedenström, John J Videler, and Johan L Van Leeuwen. How swifts control their glide performance with morphing wings. *Nature*, 446(7139):1082, 2007.

[4] Brett Klaassen van Oorschot, Emily A Mistick, and Bret W Tobalske. Aerodynamic consequences of wing morphing during emulated take-off and gliding in birds. *Journal of Experimental Biology*, pages jeb–136721, 2016.

[5] Anna Carruthers, Graham Taylor, Simon Walker, and Adrian Thomas. Use and function of a leading edge flap on the wings of eagles. In *45th AIAA Aerospace Sciences Meeting and Exhibit*, page 43, 2007.

[6] Rudolf Dvořák. Aerodynamics of bird flight. In *EPJ Web of Conferences*, volume 114, page 01001. EDP Sciences, 2016.

[7] Daniel Grant, Mujahid Abdulrahim, and Rick Lind. Flight dynamics of a morphing aircraft utilizing independent multiple-joint wing sweep. In *AIAA Atmospheric Flight Mechanics Conference and Exhibit*, page 6505, 2006.

[8] John Flanagan, Rolf Strutzenberg, Robert Myers, and Jeffrey Rodrian. Development and flight testing of a morphing aircraft, the nextgen mfx-1. In *48th AIAA/ASME/ASCE/AHS/ASC Structures, Structural Dynamics, and Materials Conference*, page 1707, 2007.

[9] AA Wissa, Y Tummala, JE Hubbard Jr, and MI Frecker. Passively morphing ornithopter wings constructed using a novel compliant spine: design and testing. *Smart Materials and Structures*, 21(9):094028, 2012.

[10] Amanda K Stowers and David Lentink. Folding in and out: passive morphing in flapping wings. *Bioinspiration & biomimetics*, 10(2):025001, 2015.

[11] The RoboSwift Team. *RoboSwift*, (accessed 28 July 2018).

[12] Alireza Ramezani, Xichen Shi, Soon-Jo Chung, and Seth Hutchinson. Bat bot (b2), a biologically inspired flying machine. In *Robotics and Automation (ICRA), 2016 IEEE International Conference on*, pages 3219–3226. IEEE, 2016.

[13] Matthew Keennon, Karl Klingebiel, and Henry Won. Development of the nano hummingbird: A tailless flapping wing micro air vehicle. In *50th AIAA aerospace sciences meeting including the new horizons forum and aerospace exposition*, page 588, 2012.

[14] M Percin. *Aerodynamic mechanisms of flapping flight*. PhD thesis, TU Delft, Delft University of Technology, 2015.

[15] Frederik Leys, Dominiek Reynaerts, and Dirk Vandepitte. Outperforming hummingbirds load-lifting capability with a lightweight hummingbird-like flapping-wing mechanism. *Biology open*, 5(8):1052–1060, 2016.

[16] Christophe De Wagter, Matej Karásek, and Guido de Croon. Quad-thopter: Tailless flapping wing robot with 4 pairs of wings. *9th international micro air vehicles*, 2017.

[17] Guido CHE de Croon, MA Groen, Christophe De Wagter, Bart Remes, Rick Ruijsink, and Bas W van Oudheusden. Design, aerodynamics and autonomy of the delfly. *Bioinspiration & biomimetics*, 7(2):025003, 2012.

[18] G. C. H. E. de Croon, Mustafa Percin, B. D. W. Remes, Rick Ruijsink, and C. De Wagter. *The DelFly - Design, Aerodynamics, and Artificial Intelligence of a Flapping Wing Robot*. Springer Netherlands, 2016.

[19] R.M.J. Janssen. Attitude control- and stabilisation moment generation of the delfly using wing tension modulation, 2016.

[20] JV Caetano, M Percin, BW van Oudheusden, B Remes, C De Wagter, GCHE de Croon, and CC de Visser. Error analysis and assessment of unsteady forces acting on a flapping wing micro air vehicle: free flight versus wind-tunnel experimental methods. *Bioinspiration & biomimetics*, 10(5):056004, 2015.

[21] Matěj Karásek. *Robotic hummingbird: Design of a control mechanism for a hovering flapping wing micro air vehicle*. PhD thesis, Universite Libre de Bruxelles, 2014.

[22] Bo Cheng and Xinyan Deng. Translational and Rotational Damping of Flapping Flight and Its Dynamics and Stability at Hovering. *IEEE Transactions on Robotics*, 27(5):849–864, oct 2011.